

# Effect of Using Internal Steel Plates for Shear Reinforcement on Flexural Behavior of Self-Compacting Concrete Beams

**Amer M. Ibrahim**

University Presidency  
University of Diyala

**Zeyad S. M. Khaled**

Dept. of Civil Eng.  
College of Engineering  
Al-Nahrain University

**Iman M. Abdul Ameer**

Dept. of Civil Eng.  
College of Engineering  
Al-Nahrain University

## Abstract

This research was conducted to investigate the effect of using internal steel plates for shear reinforcement on flexural behavior of SCC beams instead of using traditional reinforcement bars (stirrups) and to study the effect of their spacing and thickness on strength. The experimental work included destructive tests on six SCC beams under two-point load. The results showed that the yield loads in all of the beams with steel plates were lower than the reference beam by (5.21%) on average, the deflection at yield load was higher by (13.72%) on average and the ultimate loads were lower by (6.77%) on average except in one beam where it was higher by (0.37%). It was also found that the ultimate deflection in beams with internal shear steel plates was lower by (10.01%) on average except in the aforementioned beam where it was higher by (2.31%). Ductility in all beams with steel plates was lower by (20.08%) on average and the strain before a load of (200kN) was higher in the longitudinal reinforcement and lower in shear steel plates and vice versa after a load of (200kN). Theoretical analysis was also carried out for all beams using the finite element program ANSYS (version 15) where theoretical results of load versus mid-span deflection relations, longitudinal reinforcement strain, shear reinforcement strain, variations of neutral axis depths and cracks patterns showed good agreement with experimental ones. Finally, some specific further studies were recommended.

**Keywords:** Shear steel plates, Self-compacting concrete, and Shear reinforcement.

## 1. Introduction

The aim of shear reinforcement in structural concrete elements is to increase ductility thus prohibit sudden failure in shear. Diagonal shear cracks usually begin near the supports and extend towards the compression zone. Any form of steel reinforcement that intersects these diagonal cracks might withstand shear forces to a certain extent where traditional shear reinforcement is usually provided in three forms; traditional steel reinforcement bars (stirrups), inclined bent-up bars and a combination of both[1]. Stirrups are the most commonly used shear reinforcement for beams. In order to resist higher shear stresses, the number of stirrups is increased having their spacing reduced and/or

their diameter increased. Some attempts have been made to find out new techniques for shear reinforcement. One of these new techniques is the use of swimmer bars. Swimmer bars are small inclined bars with both ends bent horizontally for a short distance welded, bolted, or spliced to both top and bottom longitudinal reinforcement[2]. Using internal steel plates for shear reinforcement of concrete beams is a new technique being investigated in this research for the first time in Iraq and for the second time on international scale. No previous research about this technique was founded before the inception of this research except Al, S. J. et al.[3]. In order to ensure the flow of concrete through the holes of the steel plates, self-compacting concrete (SCC) was used in this research. It has been developed in Japan by Okamura in the late (1980s) to be mainly used for highly congested reinforced concrete structures in seismic regions. Since then it has been paid tremendous interest among the research scholars, engineers and concrete technologists[4]. It is a new type of concrete which has the ability to flow under its own weight and spread into place to completely fill molds flowing around dense reinforcement without any blocking effect or the need of vibration[5]. It has proved to be more economical with improved quality of the final product especially because it induces faster construction, reduction in site manpower, better surface finishes, easier placing, improved durability, absence of vibration and enhancement of mechanical properties (e.g. compressive strength, flexural strength, and modulus of elasticity)[6].

## 2. Research Objectives

The objectives of this research is to investigate the possibility of using internal shear steel plates, with different spacing and thicknesses, instead of stirrups by studying the strength of SCC beams and cracks behavior under flexural failure.

## 3. Research Justification

The effect of using internal steel plates for shear reinforcement on shear strength of concrete beams was already studies once by Al, S. J. et al.[3]. What is still questionable is the effect of using internal shear steel plates on flexural behavior of the beam because they might partition it into parts.

**4. Experimental Work**

**4.1 Beams Preparation**

Six simply supported concrete beams with the same rectangular cross section of (0.3m×0.2m) and the same overall length of (2m) were prepared. The beams were tested under two-point load where they were designed to fail in flexure according to ACI 318M-14[7]. A reference beam (B1) was prepared using traditional stirrups of (Ø10mm) while the other beams (B2 to B6) were prepared using shear steel plates with different spacing and thicknesses to study the effect of their use on the strength of concrete beams and cracks behavior. Table (1) shows details of these beams. Steel bars of (3Ø16mm) were used for longitudinal flexure reinforcement at the bottom of all beams, while steel bars of (2Ø10mm) was used for longitudinal reinforcement at the top of the beams. The average yield and ultimate stresses and elongations of the steel reinforcement bars are listed in Table (2). The shape of steel plates used is shown in Plate (1) and their dimensions are shown in Fig. (1). Table (3) illustrates the yield and ultimate tensile strengths of the steel plates in addition to related elongations. The materials used to produce SCC beams were: Ordinary Portland cement, sand, crushed gravel of maximum size of (10mm), clean tap water, mineral admixture in the form of metakaolin and superplasticizer known as High Water Reducing Agent (HWRE) which is a new generation of modified polycarboxylic ether that is free from chlorides and complies with ASTM C494-15[8].

**Table 1:** Shear reinforcement details for all beams

Beams	Reinforcement	Thickness	Spacing
B <sub>1</sub>	Stirrups	*	200 mm
B <sub>2</sub>	Steel plates	4mm	200 mm
B <sub>3</sub>	Steel plates	4mm	175 mm
B <sub>4</sub>	Steel plates	4mm	150 mm
B <sub>5</sub>	Steel plates	6mm	200 mm
B <sub>6</sub>	Steel plates	3mm	200 mm

\* Steel bars of Ø10 mm were used.



**Plate 1:** Shape of Steel plates used

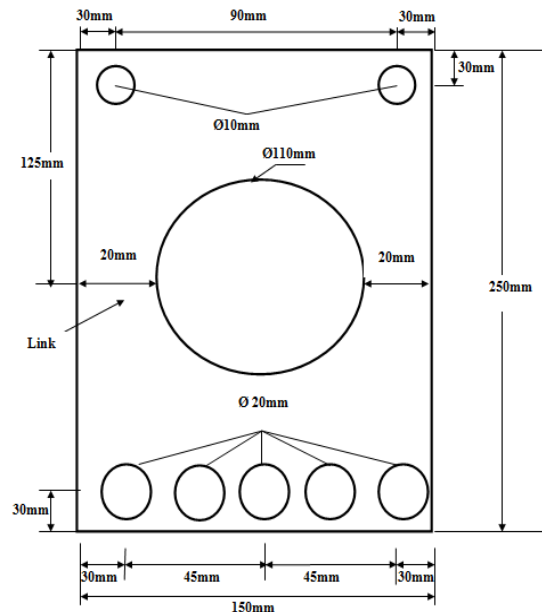


**Figure 1:** Dimension of steel plates used

**Table 2:** Yield and ultimate stresses and elongations of steel bars

Nominal bar diameter (mm)	Bar cross area (mm <sup>2</sup> )	Yield stress (MPa)	Ultimate stress (MPa)	% Elongation at ultimate stress
16	201.06	415	644	23.82
10	78.54	360	485	20.37

**Table 3:** Yield and ultimate tensile strengths and elongations of the steel plates

Thickness of steel plates (mm)	Average yield tensile strength (MPa)	Average ultimate tensile strength (MPa)	% Elongation at ultimate stress
6	230	355	27%
4	260	385	24%
3	290	375	20.5%

The whole length of longitudinal flexure reinforcement was (2010mm) having an effective length of (1900mm) where the remaining length was bended at (90°) as standard hooks of (100mm) length equally at both ends. The reference beam (B1) was reinforced with stirrups which were bended at (90°) as standard hooks as shown in Plate (2). In the others beams (B2 to B9) shear steel plates were used instead of stirrups as in the example shown in Plate (3). The steel reinforcement was already fixed in place before the SCC mix was prepared and poured in the molds. After casting is finished the beams were covered with canvas and sprinkled continuously with water for (28days).

**4.2 Control Specimens**

Properties of the SCC in both fresh and hardened states were tested using standard methods and specimens. SCC fresh state tests

included; slump flow and ( $T_{5D}$  cm) test and L-box test. SCC hardened state tests included; compressive strength, modulus of rupture splitting tensile strength and modulus of elasticity.



Plate 2: Steel cage of beam ( $B_1$ )



Plate 3: Steel cage of beam ( $B_2$ )

### 4.3 Test Instrumentation

The strain gauges used were type PFL-30-11-3L from TML to measure the evolution of strain in steel and concrete due to applied loads. The steel reinforcement was instrumented with five strain gauges immersed in the concrete with another strain gauge fixed on the middle top surface of the concrete beam. In beams ( $B_1$ ,  $B_2$ ,  $B_5$ , and  $B_6$ ) the four immersed strain gauges were distributed inside the beam at the middle region of the shear reinforcement limbs as shown in Plate (4).

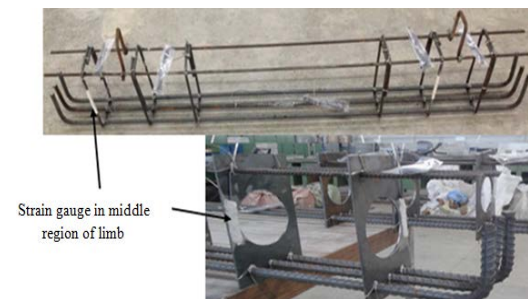


Plate 4: Strain gauges locations

These gauges were fixed at (100mm) and (300mm) from both left and right supports as shown in Fig. (2), where the sign (x) refers to the locations of gauges.

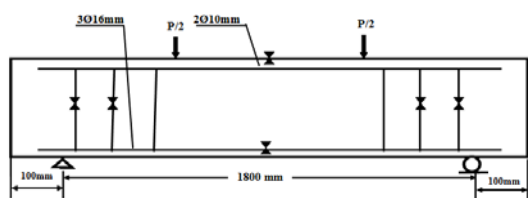


Figure 2: Locations of strain gauges in  $B_2$ ,  $B_5$  and  $B_6$

In beam ( $B_3$ ) the four immersed strain gauges were allocated inside the beam at the middle of the shear reinforcement limbs at (212.5mm) and (387.5mm) from both left and right supports. In

beam ( $B_4$ ) the four immersed strain gauges were allocated inside the beam at the middle of the shear reinforcement limbs at (225mm) and (375mm) from both left and right supports. Finally, in all beams, one immersed strain gauge was fixed at the bottom surface of the middle lower longitudinal reinforcement bar (900mm) from both supports. When the standard curing period is over, the beams were extracted and left to dry then painted in white pigment. All beams were tested using a hydraulic universal testing machine of (2000kN) capacity as shown in Plate (5).



Plate 5: Position of beams in the load testing machine

A micro crack meter device was used to measure the development of cracks widths at all stages of loading. The device has a measuring range of (4mm) with precision of (0.02mm). Three vertical dial gauges were used to measure the deflection of the tested beams. One is positioned at the center of beam and the two others at (300 mm) away from both sides of the center. These dial gauges have a maximum measurement of (5mm) and precision of (0.01mm).

## 5. Discussion of Results

### 5.1 Yield load

Table (4) presents the values of yield loads corresponding to the yield strains obtained using shear steel plates with equivalent cross sectional area at the narrowest part of the steel plate limbs. It is clear that the yield load of the longitudinal reinforcement in the beams with shear steel plates was less than the reference beam ( $B_1$ ). This is due to the centralization of stresses in the middle part of the beam because of the interlocking effect between shear steel plates and the longitudinal reinforcement causing some decrease and delay in cracks formation and stress development in both sides of the concrete beam. Subsequently the cracks increased in the middle part of the beam accompanied with a raise in the neutral axis and a decrease in the depth of the compression zone where the cracked moment of inertia decreased. Thus, strain in the middle part had increased while it had decreased in the other parts. It was also found that the yield load had decreased as the spacing between shear steel plates was decreased because the plates became closer to each other providing more interlocking effect with the longitudinal reinforcement.

**Table 4:** Strength and ductility characteristics of all beams

Beams	*P <sub>y</sub> (kN)	% diff. of P <sub>y</sub>	P <sub>u</sub> (kN)	% diff. of P <sub>u</sub>	**Δ <sub>y</sub> (mm)	% diff. of Δ <sub>y</sub>	Δ <sub>u</sub> (mm)	% diff. of Δ <sub>u</sub>	Ductility	% diff. of ductility
B1	165		266	-----	7.48	-----	37.48	-----	5.01	-----
B2	161	-2.42	242	-9.09	8.92	+16.14	32.92	-12.17	3.69	-26.34
B3	157	-4.85	267	+0.37	9.32	+19.72	38.37	+2.31	4.12	-17.76
B4	150	-9.09	260	-2.26	8.34	+10.31	36.42	-2.83	4.37	-12.77
B5	155	-6.06	250	-6.02	8.36	+10.53	32.90	-12.22	3.94	-21.36
B5	159	-3.64	240	-9.77	8.37	+11.90	32.67	-12.83	3.90	-22.16

\* P<sub>y</sub>: Yield load of longitudinal reinforcement when it reached its yield strain.

\*\* Δ<sub>y</sub>: Deflection at yield load

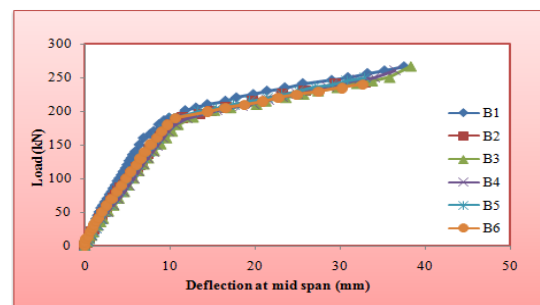
### 5.2 Ultimate Load

Table (4) also showed the values of ultimate loads obtained from load-deflection diagrams. It was found that the ultimate load in beams (B2, B4, B5 and B6) was lower than the reference beam (B1) by (9.02%) and (2.26%) respectively. This is due to the difference in yield strength between stirrups and shear steel plates. When the yield strength increases, the ultimate carrying capacity of the beam also increases. On the other hand, it was found that the ultimate load in beam (B3) was higher than the reference beam (B1) by (0.37%). This is because of the redistribution of stresses after a load of (200kN) due to strain hardening in the longitudinal reinforcement and the development of diagonal cracks in both sides of the concrete beam causing less interlocking between the plates and the longitudinal reinforcement. This brings down the neutral axis of the beam which increases the depth of the compression zone and cracked moment of inertia leading to increased ultimate load of beam (B3). It was also found that the ultimate load had increased as the thickness of the shear steel plate was increased. This is because more plate thickness enhances its shear strength (V<sub>s</sub>). Consequently the shear strength of steel and concrete (V<sub>s</sub> and V<sub>c</sub>) is raised causing diagonal shear cracks formation at the outer parts of the beam, while stresses are transferred to the middle part. This is due to the interlocking effect between longitudinal reinforcement and steel plates which increase stresses and strain in the middle part. As a result, the neutral axis is raised more, the depth of the compression zone is eventually decreased and the cracked moment of inertia is also decreased. Therefore, longitudinal reinforcement yields at lower load than in beam (B1). After cracks start to form, the strain eventually increases in the left and right parts of the beam until the plate imminently approaches to yield stage where cracks become wider and wider due to increased tensile stresses transferred to the concrete. This leads to redistribution of strain in the longitudinal reinforcement causing the neutral axis to drop down and the depth of the compression zone and cracked moment of inertia to increase; hence this influences the ultimate

load and ultimate strain. This was noticed after the load exceeded (200kN) despite the difference in yield strength between plates and stirrups.

### 5.3 Load-Deflection Behavior

The values of deflection at yield and ultimate loads obtained from the dial gauge readings were also shown in Table (4). It was found that the deflection at yield load in beams with shear steel plates was higher than the reference beam (B1) for the reason explained in (5.1). It was also found that the deflection at ultimate load in beams (B2, B4, B5 and B6) was less than the reference beam (B1). This is due to the redistribution of stresses because of strain hardening which occurs in the longitudinal reinforcement and brings down the neutral axis of the beam so increases the depth of the compression zone and cracked moment of inertia. On the other hand, the deflection in beam (B3) was higher than the reference beam (B1) by (2.31%) for the reason explained in (5.2). It can be noticed from Fig. (3) that the deflection at yield and ultimate loads was close in all beams because the beams were designed to fail in flexure.



**Figure 3:** Load-deflection curves of all beams at mid span

### 5.4 Ductility

Table (4) also showed that the ductility (Δ<sub>u</sub>/Δ<sub>y</sub>) in beams with shear steel plates is less than the reference beam (B1). This is because the deflection at the ultimate load had decreased for the reason explained in (5.3). On the other hand, the deflection at yield load had increased for the reason explained in (5.1).

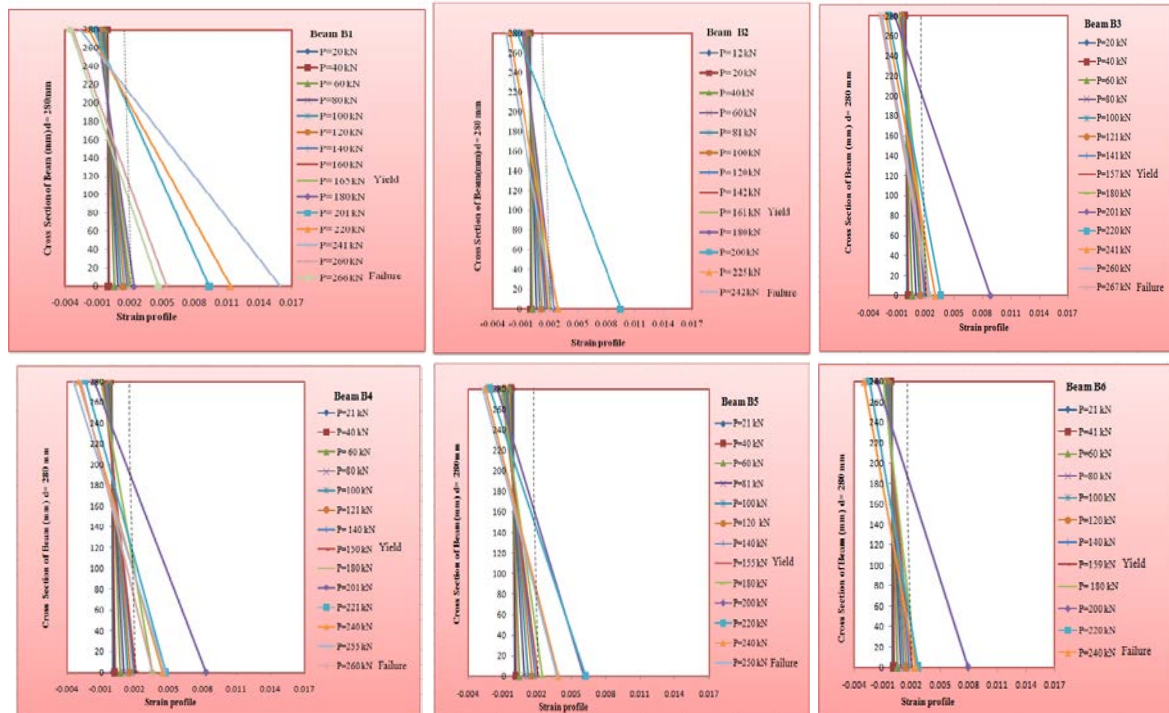
### 5.5 Strain Characteristics in the Longitudinal Reinforcement

Table (5) shows the values of strain at the midpoint of the longitudinal reinforcement under different loads (120, 140, 150 and 210kN) obtained by strain gauges connected to the data logger. It was found that the strain in the longitudinal reinforcement under the loads (120, 140 and 150kN) was higher than the strain in the reference beam (B1). This is due to the reason explained in (5.1). It can also be noticed from

Table (5) that the strain in the longitudinal reinforcement increased as spacing between shear steel plates decreased. This is also due to the reason explained in (5.1). It can also be noticed from Table (5) that strain in the longitudinal reinforcement increased as the thickness of shear steel plates was increased for the reason explained in (5.2), while the strain under the load of (210kN) was less than the reference beam (B1) also for the reason explained in (5.2). The strain profiles of the beams are shown in Fig. (4).

**Table 5:** Strain characteristics in the longitudinal reinforcement of beams

Beams	$\epsilon \times 10^{-3}$ at load 120 kN	% diff. of $\epsilon$ at load 120 kN	$\epsilon \times 10^{-3}$ at load 140 kN	% diff. of $\epsilon$ at load 140 kN	$\epsilon \times 10^{-3}$ at load 150 kN	% diff. of $\epsilon$ at load 150 kN	$\epsilon \times 10^{-3}$ at load 210 kN	% diff. of $\epsilon$ at load 210 kN
B1	1.461	-----	1.741	-----	1.868	-----	10.660	-----
B2	1.523	+4.07	1.802	+3.39	1.951	+4.25	6.119	-42.60
B3	1.542	+5.25	1.853	+6.04	1.923	+2.86	5.941	-44.27
B4	1.603	+8.86	1.880	+7.39	2.060	+9.32	4.942	-53.64
B5	1.547	+5.56	1.860	+6.40	2.006	+6.87	6.156	-42.25
B6	1.492	+2.08	1.786	+2.52	1.909	+2.15	5.300	-50.28



**Figure 4:** Strain profile of longitudinal reinforcement and compression face of concrete beams

### 5.6 Strain Characteristics in Shear Reinforcement at Both Sides of Beams

Tables (6 and 7) show the strain values in shear reinforcement (both stirrups and steel plates) in the right and left sides of the beams under the loads (120, 140, 150 and 210kN) obtained from strain gauges connected to the data logger. It was found that the strain in shear steel plates at the right and left sides of the beams under the loads (120, 140 and 150kN) were less

than the reference beam (B1). This is due to the reason explained in (5.1). It can also be noticed from these tables that the strain in shear steel plates had decreased as spacing between them decreased, also for the reason explained in (5.1). Furthermore, the strain in shear steel plates had decreased as the thickness of shear steel plates was increased. This is because the increased area of steel plates brings down the stress and its equivalent strain, while the strain under the load of (210kN) was more than the reference beam (B1) for the reason explained in (5.5).

**Table 6:** Strain characteristics in shear reinforcement at right side of beams

Beams	$\epsilon \times 10^{-3}$ at load 120 kN	% diff. of $\epsilon$ at load 120 kN	$\epsilon \times 10^{-3}$ at load 140 kN	% diff. of $\epsilon$ at load 140 kN	$\epsilon \times 10^{-3}$ at load 150 kN	% diff. of $\epsilon$ at load 150 kN	$\epsilon \times 10^{-3}$ at load 210 kN	% diff. of $\epsilon$ at load 210 kN
B1	0.666	-----	0.718	-----	0.805	-----	1017	-----
B2	0.423	-36.48	0.497	-30.78	0.610	-24.22	1230	+17.32
B3	0.398	-40.24	0.472	-34.26	0.596	-25.96	1270	+24.88
B4	0.379	-43.09	0.418	-41.78	0.507	-37.02	1497	+47.20
B5	0.388	-41.74	0.452	-37.05	0.538	-33.17	1201	+15.32
B6	0.494	-25.83	0.538	-25.07	0.621	-22.86	1480	+31.28

**Table 7:** Strain characteristics in shear reinforcement at left side of beams

Beams	$\epsilon \times 10^{-3}$ at load 120 kN	% diff. of $\epsilon$ at load 120 kN	$\epsilon \times 10^{-3}$ at load 140 kN	% diff. of $\epsilon$ at load 140 kN	$\epsilon \times 10^{-3}$ at load 150 kN	% diff. of $\epsilon$ at load 150 kN	$\epsilon \times 10^{-3}$ at load 210 kN	% diff. of $\epsilon$ at load 210 kN
B1	0.690	-----	0.791	-----	0.857	-----	1018	-----
B2	0.494	-28.41	0.513	35.15	0.603	-29.64	1300	+21.69
B3	0.435	36.96	0.486	38.56	0.611	28.70	1330	+23.46
B4	0.417	39.57	0.452	42.86	0.557	35.00	1510	+32.58
B5	0.381	-44.78	0.471	-40.46	0.588	-31.39	1218	+16.42
B6	0.497	-27.97	0.569	-28.07	0.654	-23.69	1435	+29.06

**5.7 Cracks Patterns**

Cracks patterns in all beams at different stages of loading are shown in Plates (6 to 11). These plates are put together with figures (8 to 13) later on for comparison sake. From these plates it can be noticed that the sequence of cracks formation started randomly in the middle third of the beams at the bottom face then they grew upward with the increased applied load. Cracks forming in the middle third of the beams were nearly vertical due to pure moment applied on this zone of the beam. On the other hand, nearly (45°) inclined cracks initiated in both sides of the beams being more inclined as being farther away of the middle zone due to the presence of shear forces in addition to moment.

Although Al, S. J. et al.[3] studied the use of internal steel plates for shear reinforcement in wide beams, the cracks patterns were almost the same as noticed in this research for the same reasons explained in (5.1), (5.2) and (5.5). When swimmer bars were used by Asha et al.[1] and Al-Nasra et al.[2] as shear reinforcement in concrete beams, the cracks patterns noticed seem to be nearly similar too. This is because swimmer bars are welded, bolted, or spliced to both top and bottom flexural steel reinforcement and have the similar effect of shear plane-crack interceptor system of shear plates instead of bar-crack interceptor system of stirrups.

**5.8 Width of First Crack at Yield Load**

Table (8) shows the width of the first crack at yield load of longitudinal reinforcement in each beam when it reached its yield strain. It was found that the first crack width in beams with shear steel plates was higher than the reference beam (B1) due to the reason explained in (5.1).

**Table 8:** First crack width in all beams

Beams	1 <sup>st</sup> Crack at yield load		% diff. of width
	Load (kN)	Width (mm)	
B <sub>1</sub>	165	0.29	-----
B <sub>2</sub>	161	0.36	+19.44
B <sub>3</sub>	157	0.34	+14.71
B <sub>4</sub>	150	0.38	+23.68
B <sub>5</sub>	155	0.36	+19.44
B <sub>6</sub>	159	0.32	+9.38

**5.9 Variation in the Neutral Axis Depth**

The locations of the neutral axes were established according to the strain recorded at the mid-span of the uppermost compression fiber of the concrete beam in coincidence with the strain recorded at the opponent position in the bottom longitudinal reinforcement. The variation in the neutral axis depth (c/d) against the variation in the applied load on the beams is illustrated in Fig. (5) where (c) is the depth of compression zone and (d) is the effective depth of the concrete beam. It is clear that the neutral axis depth in beams with the shear steel plates was lower than that in the reference beam (B1) due to the reason explained in (5.1). It is also clear that the neutral axis raised more as the spacing between shear steel plates was decreased or the thickness of shear steel plate was increased due to the reason explained in (5.2).

It can be noticed in Fig (5) that the neutral axis depths initially decreased then nearly stabilized until yield load was reached. After reaching the load of (200kN), the neutral axis depths increased as a reduction happened in the compression area due to redistribution of strain in the longitudinal reinforcement made by the constraints made by the holes of the shear steel

plates which caused its strain to increase, so the neutral axis went upward gradually in the middle third region until the beam suddenly failed.

**6. Comparison between Experimental and Finite Element Models Results**

The finite element method was used in order to verify the experimental results of reinforced concrete beams compared to theoretical results. The characteristics of the finite elements used in modeling each of the tested beams using ANSYS program (version 15) are summarized in Table (9).

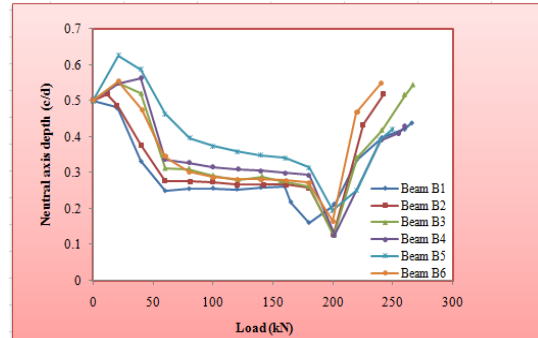


**Figure 5:** Variation of neutral axis depth of beams

**Table 9:** Characteristics of finite elements used (\* From ANSYS Library.)

Beam components	Element Type*	Element Representation
Concrete	SOLID65	8-node Brick Element (3 Translation DOF per node)
Steel Reinforcement Bars	LINK180	2-node Discrete Element (3 Translation DOF per node)
Shear Steel Plates	SHELL281	8-node shell element (3 Translation DOF per node)
Loading Bearing Plate	SOLID185	8-node Brick Element (3 Translation DOF per node)

**6.1 Load-Deflection Behavior**

Results of load versus mid-span deflection relations obtained from the ANSYS models were compared to the experimental load versus mid-span deflection as shown in Fig. (6). Good agreement can be noticed between experimental and theoretical results. It can also be noticed that theoretical load-deflection behavior was stiffer at the first stage of loading than the experimental one. Then the experimental load-deflection behavior became stiffer than theoretical one. This is due to the restriction on the degree of freedom which increases the stiffness and subsequently leads to load increase and deflection decrease. Therefore, it is noticed that theoretical ultimate loads were higher than the experimental ones and theoretical ultimate deflections were lower than

the experimental ones. Tables (10 and 11) list the theoretical and experimental results of yield load, deflection at yield load, ultimate load and maximum mid-span deflection at ultimate load. These differences between experimental and theoretical results existed due the fact that the program is designed to work under perfect conditions which is not the case in real life work.

**6.2 Strain Characteristics in the Longitudinal Reinforcement**

It can be noticed from Tables (12 and 13) that experimental and theoretical results of longitudinal reinforcement strain have good agreement with each other. The differences between experimental and theoretical results existed due the reason already mentioned in (6.1).

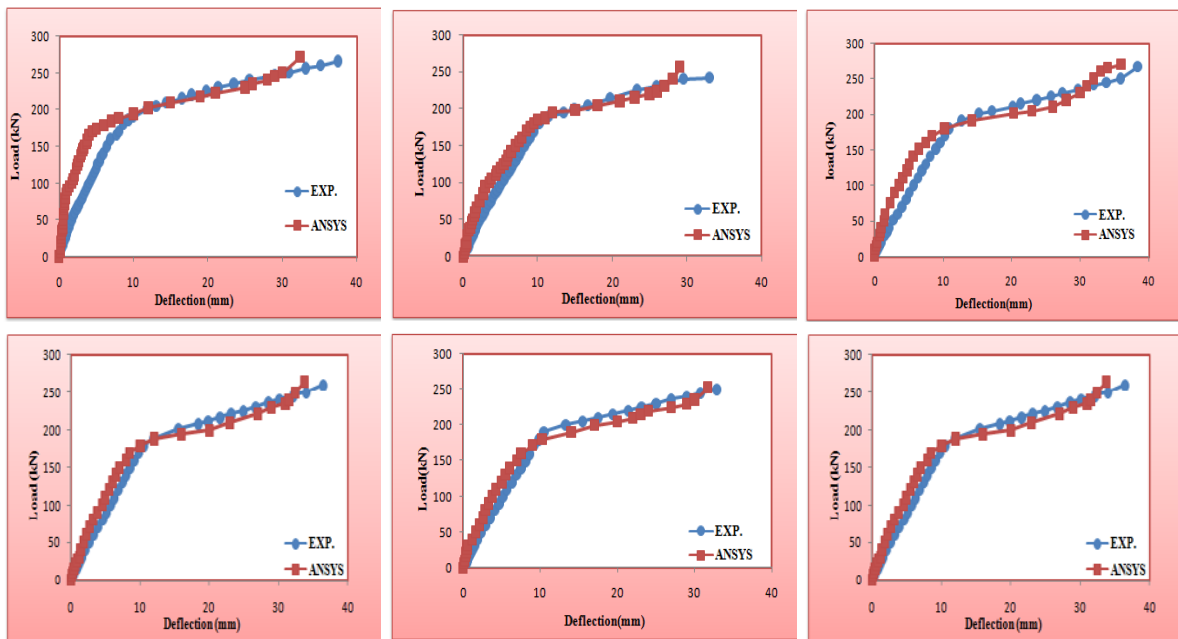


**Figure 6:** Experimental and theoretical load vs. deflection curves for all beams

**Table 10:** Experimental and theoretical results of yield loads and related deflections

Beams	Yield load $P_y$ (kN)			Mid span deflection $\Delta_y$ (mm)		
	Experiment	ANSYS	Diff%	Experiment	ANSYS	Diff. %
B <sub>1</sub>	165	170	-2.94	7.48	5.6	+25.13
B <sub>2</sub>	161	167	-3.59	8.92	8.3	+ 6.95
B <sub>3</sub>	157	160	-1.88	9.32	7.5	+19.53
B <sub>4</sub>	150	156	-3.85	8.34	7.4	+11.27
B <sub>5</sub>	155	159	-2.52	8.36	7.4	+11.48
B <sub>6</sub>	159	164	-3.04	8.37	7.3	+12.78
	Avg. of Diff%		2.97	Avg. of Diff%		14.52

**Table 11:** Experimental and theoretical results of ultimate loads and related deflections

Beams	Ultimate load $P_u$ (kN)			Mid span deflection $\Delta_u$ (mm)		
	Experiment	ANSYS	Diff%	Experiment	ANSYS	Diff. %
B <sub>1</sub>	266	272	-2.21	37.48	32.3867	+13.59
B <sub>2</sub>	242	256	-5.47	32.92	29.0312	+11.81
B <sub>3</sub>	267	270	-1.11	38.37	35.9904	+ 6.20
B <sub>4</sub>	260	265	-1.89	36.42	33.764	+7.29
B <sub>5</sub>	250	253	-1.19	32.9	31.7019	+3.64
B <sub>6</sub>	240	245	-2.04	32.67	29.6891	+9.12
	Avg. of Diff%		2.32	Avg. of Diff%		8.61

**Table 12:** Strain characteristics of longitudinal reinforcement under the loads (120 and 140kN)

Beams	$\epsilon \times 10^{-3}$ at load 120 kN			$\epsilon \times 10^{-3}$ at load 140 kN		
	Experiment	ANSYS	Diff%	Experiment	ANSYS	Diff. %
B <sub>1</sub>	1.461	1.334	+8.69	1.741	1.553	+10.80
B <sub>2</sub>	1.523	1.402	+7.94	1.802	1.697	+5.83
B <sub>3</sub>	1.542	1.459	+5.38	1.853	1.714	+7.50
B <sub>4</sub>	1.603	1.549	+3.36	1.880	1.748	+7.02
B <sub>5</sub>	1.547	1.503	+2.84	1.860	1.723	+7.37
B <sub>6</sub>	1.492	1.366	+8.44	1.786	1.538	+13.89
	Avg. of Diff%		6.11	Avg. of Diff%		8.74

**Table 13:** Strain characteristics of longitudinal reinforcement under the loads (150 and 210kN)

Beams	$\epsilon \times 10^{-3}$ at load 150 kN			$\epsilon \times 10^{-3}$ at load 210 kN		
	Experiment	ANSYS	Diff%	Experiment	ANSYS	Diff. %
B <sub>1</sub>	1.868	1.668	+10.71	10.660	9.523	+10.67
B <sub>2</sub>	1.951	1.775	+9.02	6.119	5.960	+2.59
B <sub>3</sub>	1.923	1.844	+4.12	5.941	5.388	+9.31
B <sub>4</sub>	2.060	1.898	+7.86	4.942	4.772	+3.44
B <sub>5</sub>	2.006	1.795	+10.52	6.156	5.993	+2.65
B <sub>6</sub>	1.909	1.703	+10.79	5.300	5.120	+3.40
	Avg. of Diff%		8.84	Avg. of Diff%		5.34

### 6.3 Strain Characteristics in Shear Reinforcement at Both Sides of Beam

It can be noticed from Tables (14 and 15) that the results of shear reinforcement strain obtained by experimental and ANSYS model results show good agreement too. The differences between experimental and theoretical results existed due the reason already mentioned in (6.1).

### 6.4 Location of the Neutral Axis

Locations of the neutral axis were established using the strain values obtained by ANSYS at mid of span on the extreme compression fiber of the concrete beam top surface and the strain at the opponent position of the bottom longitudinal reinforcement. Variations in the neutral axis

depths obtained from the ANSYS model were compared to the corresponding experimental variations of neutral axis depths where good agreement was observed between experimental and theoretical results. It can be noticed from Fig. (7) that the neutral axis locations in the ANSYS models show stiffer behavior at all stages of loading than the neutral axis locations in experimental work due the reason already mentioned in (6.1).

### 6.5 Cracks Patterns

The comparison of the concrete fracture patterns at failure of all beams as resulted from experimental tests with those theoretically predicted using ANSYS models showed good agreement as shown in Figs. (8 to 13).

**Table 14:** Strain characteristics of shear reinforcement under the loads (120 and 140kN)

Beams	$\epsilon \times 10^{-3}$ at load 120 kN			$\epsilon \times 10^{-3}$ at load 140 kN		
	Experiment	ANSYS	Diff%	Experiment	ANSYS	Diff. %
B <sub>1</sub>	0.678	0.619	+8.70	0.755	0.704	+6.75
B <sub>2</sub>	0.459	0.447	+2.61	0.505	0.543	-6.10
B <sub>3</sub>	0.417	0.419	-0.47	0.479	0.519	-7.71
B <sub>4</sub>	0.398	0.386	+3.05	0.435	0.479	-9.19
B <sub>5</sub>	0.385	0.351	+8.83	0.462	0.453	+1.95
B <sub>6</sub>	0.496	0.499	-0.60	0.554	0.601	-7.82
	Avg. of Diff%		4.04	Avg. of Diff%		6.59

**Table 15:** Strain characteristics of shear reinforcement under the loads (150 and 210kN)

Beams	$\epsilon \times 10^{-3}$ at load 150 kN			$\epsilon \times 10^{-3}$ at load 210 kN		
	Experiment	ANSYS	Diff%	Experiment	ANSYS	Diff. %
B <sub>1</sub>	0.831	0.749	+9.86	1.018	0.970	+4.72
B <sub>2</sub>	0.607	0.605	+0.33	1.265	1.115	+11.86
B <sub>3</sub>	0.604	0.583	3.48	1.300	1.203	+7.62
B <sub>4</sub>	0.532	0.528	+0.75	1.504	1.347	+10.44
B <sub>5</sub>	0.563	0.559	+0.71	1.210	1.104	+8.76
B <sub>6</sub>	0.638	0.615	+3.61	1.458	1.326	+9.05
	Avg. of Diff%		3.12	Avg. of Diff%		8.74

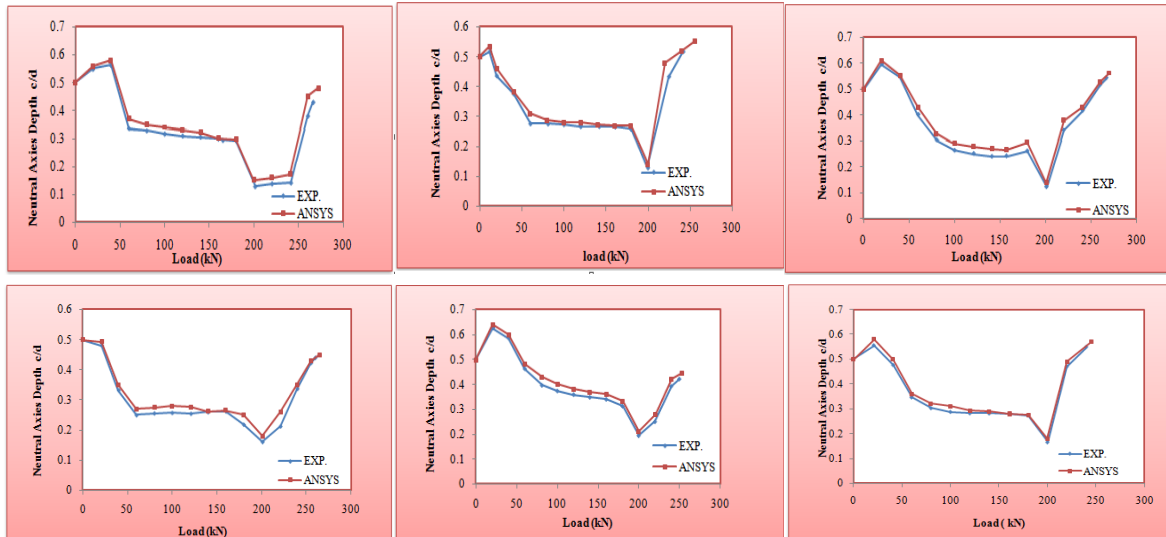


**Figure 7:** Experimental and theoretical variation of neutral axis depth of beams



**Plate 6:** Cracks patterns in beam (B<sub>1</sub>)

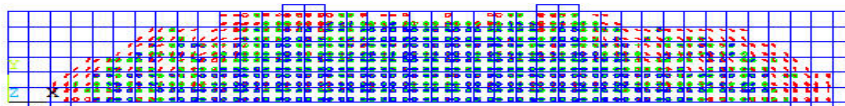


**Figure 8:** Theoretical concrete cracks patterns in beam (B<sub>1</sub>)



**Plate 7:** Cracks patterns in beam (B<sub>2</sub>)

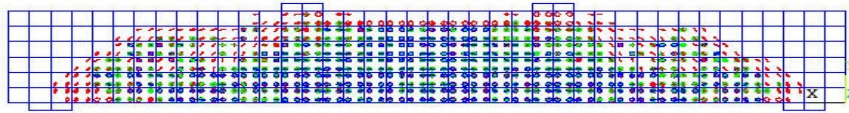


**Figure 9:** Theoretical concrete cracks patterns in beam (B<sub>2</sub>)

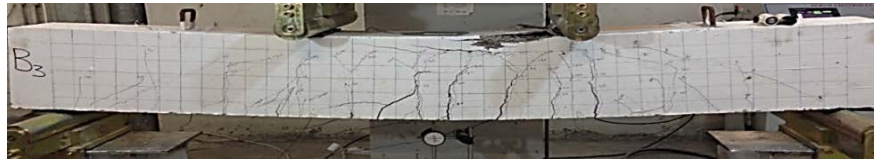


**Plate 8:** Cracks patterns in beam (B<sub>3</sub>)

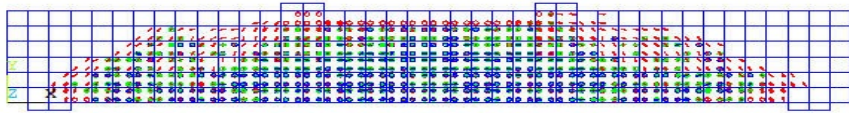


**Figure 10:** Theoretical concrete cracks patterns in beam (B<sub>3</sub>)

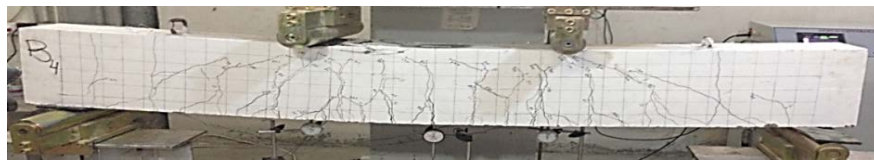


**Plate 9:** Cracks patterns in beam (B<sub>4</sub>)

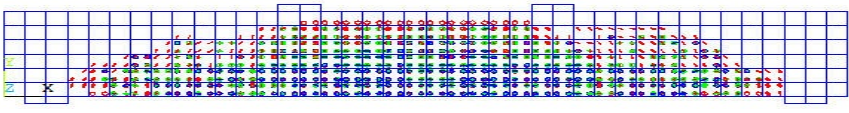


**Figure 11:** Theoretical concrete cracks patterns in beam (B<sub>4</sub>)



**Plate 10:** Cracks patterns in beam (B<sub>5</sub>)

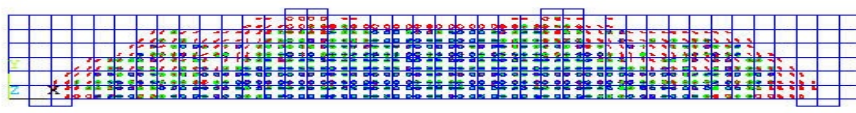


**Figure 12:** Theoretical concrete cracks patterns in beam (B<sub>5</sub>)



**Plate 11:** Cracks patterns in beam (B<sub>6</sub>)



**Figure 13:** Theoretical concrete cracks patterns in beam (B<sub>6</sub>)

**7. Conclusions**

Based on the experimental and theoretical results of this research, the following conclusions were drawn:

- i. The yield load in beams using internal shear steel plates was lower than the reference beam using stirrups by an average of (5.21%).
- ii. The deflection at yield load in beams using internal shear steel plates was higher than the reference beam using stirrups by an average of (13.72%) which is a very noticeable difference.
- iii. The ultimate load in beams using internal shear steel plates was lower than the reference beam using stirrups by an average

- of (6.77%) except in beam (B3) where it was higher by (0.37%).
- iv. The ultimate deflection in beams using internal shear steel plates was lower than the reference beam using stirrups by an average of (10.01%) except in beam (B3) where it was higher by (2.31%).
  - v. Ductility in all beams using internal shear steel plates was lower than the reference beam using stirrups by an average of (20.08%).
  - vi. The use of thicker steel plates led to noticeable increase in the ultimate carrying capacity of the beams even when the yield strength of shear steel plates was lower than stirrups.
  - vii. The strain in all beams using internal shear steel plates before reaching the load of (200kN) tended to increase in the longitudinal reinforcement and to decrease in the steel plates then vice versa after the load of (200kN).
  - viii. The finite element model developed using ANSYS (version 15) program was able to simulate the behavior of reinforced concrete beams using internal shear steel plates.
  - ix. The theoretical analysis carried out using ANSYS showed that the curves of predicted load-deflection versus variation in the neutral axis were slightly stiffer than the experimental results for the reasons explained in (6.1 and 6.4). Nevertheless the analytical results are in good agreement with the experimental results.

## 8. Recommendations

Based on the conclusions, it can be recommended to use internal steel plates as a new technique for shear reinforcement for concrete beams. Nevertheless, further studies must be conducted. The following future studies are recommended:

- i. To study the effect of using internal steel plates for shear reinforcement on flexural behavior using more samples with different sizes and shapes.
- ii. To study the effect of using internal steel plates for shear reinforcement on shear behavior using more samples with different sizes and shapes.
- iii. To study the effect of using inclined internal steel plates for shear reinforcement nearly perpendicular to cracks patterns.
- iv. To investigate the variation in work productivity (erection time and effort) entailed when using internal shear steel plates compared to using stirrups.
- v. To investigate the variation in cost entailed when using internal shear steel plates compared to using stirrups.

## References

- [1] Asha, N. M., Al-Nasra, M. M., and Najmi, A. S., (2012), "Optimizing the Use of Swimmer Bars as Shear Reinforcement in the Reinforced Concrete Beams", *International Journal of Civil and Structural Engineering*, Vol. 3, No 2, p. 313-320.
- [2] Al-Nasra, M. M., and Asha, N. M., (2015), "Investigating the Use of Spliced Swimmer Bars as Shear Reinforcement in Reinforced Concrete Beams", *International Organization of Scientific Research Journal of Engineering (IOSRJEN)*, Vol. 05, No.02, p. 47-54.
- [3] Al, S. J., Ibrahim, A. M., and Agarwal, V. C., (2015) "Effect Steel Plate of Shear Reinforced Wide Beam Concrete", *International Journal of Science and Research (IJSR)*, National Institute of Science Communications and Information Resources – NISCAIR, India, Vol. 4, No.2, p. 596-601.
- [4] Ameli, M. and Ronagh, H.R., (2007), "Treatment of Torsion of Reinforced Concrete Beams in Current Structural Standards", *Asian Journal of Civil Engineering - Building and Housing*, Vol. 8, No. 5, p. 507-519.
- [5] Aggelos, S., Kosmas, K., and Nikolaos, S., (2010), "Properties of SCC Produced with Limestone Filler or Viscosity Modifying Admixture", *Journal of Materials in Civil Engineering*, ASCE, Vol. 22, No.4, p. 352-360.
- [6] European Federation of National Associations Representing for Concrete- EFNARC, (2005), "Specifications and Guidelines for Self-Compacting Concrete", Association House, 99 West Street, Farnham, Surrey GU9 7EN, UK, p. 31.
- [7] American Concrete Institute, ACI Committee 318, (2014), "Building Code Requirements for Structural Concrete and Commentary", ACI 318RM-14, p. 507-516.
- [8] American Society for Testing and Material, (2015), "Standard Specification for Chemical Admixtures for Concrete, ASTM-C494-15.

## تأثير استخدام صفائح الفولاذ الداخلية لتسليح القص على تصرف الانثناء في عتبات الخرسانة ذاتية الرص

إيمان ماجد عبد الأمير  
قسم الهندسة المدنية  
كلية الهندسة  
جامعة النهريين

أ.م.د. زياد سليمان محمد خالد  
قسم الهندسة المدنية  
كلية الهندسة  
جامعة النهريين

أ.د. عامر محمد إبراهيم  
رئاسة الجامعة  
جامعة ديالى

### الخلاصة

تم إجراء هذا البحث للتحري عن تأثير استخدام صفائح الفولاذ الداخلية لتسليح القص على تصرف الانثناء في العتبات الخرسانية ذاتية الرص بدلاً من قضبان التسليح التقليدية (الحلقية) ودراسة تأثير تباعدها وسمكها. وقد تضمن العمل المختبري فحص ستة عتبات خرسانية ذاتية الرص فحواً أتلافياً تحت حمل مسلط على نقطتين. وقد أظهرت النتائج أن أحمال الخضوع للعتبات ذات الصفائح الفولاذية كافة هي أقل بمعدل (5.21%) وأن الانحناء عند حمل الخضوع كان أعلى بمعدل (13.72%) وأن الأحمال القصوى كانت أقل بمعدل (6.77%) فيما عدا عتبة واحدة إذ كانت أعلى بنسبة (0.37%). كما وجد أن الانحناء الأقصى في العتبات ذات الصفائح الفولاذية كافة هو أقل بمعدل (10.01%) فيما عدا عتبة واحدة إذ كانت أعلى بنسبة (2.31%). وأن المطيلية في العتبات ذات الصفائح الفولاذية كافة هي أقل بمعدل (20.08%) وأن الانفعال قبل وصول الحمل (200 كيلو نيوتن) هي أعلى في التسليح الطولي وأقل في الصفائح الفولاذية، والحالة معكوسة بعد تخطي الحمل (200 كيلو نيوتن). وقد تم إجراء التحليل النظري لكل عتبة أيضاً باستخدام برنامج العناصر الدقيقة (ANSYS version 15) حيث أظهرت النتائج النظرية لعلاقة الحمل بالانحناء في منتصف طول العتبة توافقاً جيداً مع النتائج المختبرية. وختاماً تمت التوصية بدراسات مستقبلية محددة الهدف.